Direct probe of electrochemical pseudocapacitive pH jump at a graphene electrode

Wang, Y.K.; Seki, T.; Liu, X.; Yu, X.Q.; Yu, C.C.; Domke, K.F.; ... ; Bonn, M.

GDCh

Communications

Angewandte
Chemie
International Edition
www.angewandte.org

Direct Probe of Electrochemical Pseudocapacitive pH Jump at a Graphene Electrode**

Yongkang Wang[+], Takakazu Seki[+], Xuan Liu, Xiaoqing Yu, Chun-Chieh Yu,
Katrin F. Domke, Johannes Hunger, Marc T. M. Koper, Yunfei Chen,* Yuki Nagata,* and
Mischa Bonn*

Abstract: Molecular-level insight into interfacial water at a buried electrode interface is essential in electrochemistry, but spectroscopic probing of the interface remains challenging. Here, using surface-specific heterodyne-detected sum-frequency generation (HD-SFG) spectroscopy, we directly access the interfacial water in contact with the graphene electrode supported on calcium fluoride (CaF_2). We find phase transition-like variations of the HD-SFG spectra vs. applied potentials, which arises not from the charging/discharging of graphene but from the charging/discharging of the CaF_2 substrate through the pseudocapacitive process. The potential-dependent spectra are nearly identical to the pH-dependent spectra, evidencing that the pseudocapacitive behavior is associated with a substantial local pH change induced by water dissociation between the CaF_2 and graphene. Our work evidences the local molecular-level effects of pseudocapacitive charging at an electrode/aqueous electrolyte interface.

Water at a potentiostatically controlled electrode surface is relevant for a wide range of scientific and technological systems.[1–5] Knowledge of the structure and orientation of water at the electrode surface is an indispensable prerequisite to comprehending the mechanism of those systems. For instance, the reorganization of interfacial water molecules and their spatial arrangement are closely linked with capacitive charge storage,[3,6] and with the electron transfer mechanism across electrode/water interfaces,[2,7–11] such as in electrocatalytic water splitting,[2,7,8] and pseudocapacitive energy storage.[9–11] Nevertheless, the molecular-level insights remain enigmatic at the electrode/aqueous electrolyte interface. Probing such an electrode/aqueous electrolyte interface possesses two inherent challenges. One lies in the complexity of the water molecules and local electric field at interfaces;[12] the interfacial water molecules are heterogeneous,[13,14] and their response to the electric field is supposed to be asymmetric.[15,16] Furthermore, probing the buried interface is challenging, because the probe often cannot reach the target interface.[17–19]

To overcome the first difficulty, heterodyne-detected sum-frequency generation (HD-SFG) spectroscopy is ideal, owing to three advantages: interface specificity, molecular specificity, and additivity of the molecular response.[20–22] An SFG signal originates solely from the interface, because it naturally excludes contributions from the bulk due to the selection rule.[23,24] An SFG signal is enhanced when the infrared (IR) frequency is resonant with the molecular vibration, providing molecular specificity. Furthermore, a HD-SFG signal ($\chi^{(2)}$) is additive and thus allows us to disentangle the contributions. The separation of the contribution further enables us to compute the surface charge at the interface.[25,26]

The second difficulty can be overcome by using graphene as an electrode; graphene, an atom-thickness metal-like material, can serve as the electrode while allowing the IR light to reach the electrode surface.[16,27–30] As such, combining SFG with a graphene electrode allows us to explore the molecular-level insight into the interfacial conformations under electrified conditions.[16]

[*] Y. Wang,[+] Y. Chen
School of Mechanical Engineering, Southeast University
211189 Nanjing (China)
E-mail: yunfeichen@seu.edu.cn

Y. Wang,[+] T. Seki,[+] X. Yu, C.-C. Yu, K. F. Domke, J. Hunger, Y. Nagata, M. Bonn
Max Planck Institute for Polymer Research
Ackermannweg 10, 55128 Mainz (Germany)
E-mail: nagata@mpip-mainz.mpg.de
bonn@mpip-mainz.mpg.de

X. Liu, M. T. M. Koper
Leiden Institute of Chemistry, Leiden University
Einsteinweg 55, 2333CC Leiden (The Netherlands)

K. F. Domke
University Duisburg-Essen, Faculty of Chemistry
Universitätsstraße 5, 45141 Essen (Germany)

[+] These authors contributed equally to this work.

[**]A previous version of this manuscript has been deposited on a preprint server (https://doi.org/10.48550/arXiv.2210.02532).

Here, we perform HD-SFG measurements at the CaF$_2$-supported electrified graphene/water interface. We observe that the Im$(\chi^{(2)})$ spectra of the O–H stretching mode of water change drastically between -0.63 V and -0.03 V versus the reversible hydrogen electrode (RHE, Pd/H$_2$). We find that it is not due to the variation of charges on the graphene, but due to the charging/discharging of the CaF$_2$ substrate through a pseudocapacitive process, likely accommodated by water trapped between the CaF$_2$ and the graphene. From HD-SFG measurements at various pH conditions, we identify that the pseudocapacitive process occurs primarily due to the hydrogen evolution reaction (HER)-induced local pH change (by ≈ 5 units, even at $1\,\mu A\,cm^{-2}$ current density) at the CaF$_2$/graphene interface. This work provides molecular-level insights into the dissociation and reorganization of interfacial water on a potentiostatically controlled electrode surface and highlights the role of the pseudocapacitive processes at the interface. Our molecular-level details of the interfacial water structure and the pseudocapacitive behavior are relevant for a wide range of scientific and technological systems such as water desalination, biosensing, energy storage, and catalysis.

To understand the structure of the interfacial water on the electrified graphene surface, we measured Im$(\chi^{(2)})$ spectra in the O–H stretching mode frequency region (2900–3700 cm^{-1}) from the graphene samples on CaF$_2$ substrates in contact with 1 mM NaClO$_4$ aqueous solution. The experimental setup is shown in Figure 1A (see Section 1–2 in the Supporting Information for more details.). The data at different potentials with respect to the Pd/H$_2$ electrode are displayed in Figure 1B. At $+0.57$ V, the Im$(\chi^{(2)})$ spectrum exhibits a negative band spanning from 2950 cm^{-1} to 3550 cm^{-1}. This negative band is assigned to the O–H stretching mode of water molecules hydrogen-bonded (H-bonded) to the other water molecules, and the negative sign of this band indicates that the H-bonded O–H group points *down* (towards the bulk solution).[15,31] This negative band contribution is insensitive to the variation of the applied potential in the range of $+0.57$ V to -0.03 V.

When we decreased the potential from -0.03 V to -0.63 V, the sign of the H-bonded O–H stretching band flips from negative to positive, illustrating that the orientation of the interfacial water molecules changes from *down* to *up* (H-bonded O–H group pointing away from the bulk solution). During this transition, we further observed the appearance of a negative 3630 cm^{-1} O–H stretch peak. Since a negative peak indicates that the O–H group points *down* to the bulk solution, this peak might originate from the O–H stretch of the Ca–O–H species on the CaF$_2$ surface.[32,33] From -0.43 V to -0.63 V, both the positive H-bonded O–H stretching band and the negative Ca–O–H stretch peak were further enhanced. From -0.63 V down to -1.23 V, the Im$(\chi^{(2)})$ spectra were found to be again insensitive to the applied potentials. Note that the graphene samples were electrochemically intact during these measurements (See Supporting Information-Section 3.1). A different electrolyte, NaCl, instead of NaClO$_4$, gave similar electrochemical SFG responses (Supporting Information-Section 4).

To examine whether the variations of the Im$(\chi^{(2)})$ spectra arise from the interfacial water conformation change or surface charge change, we estimated the net surface charge (σ_{net}) at
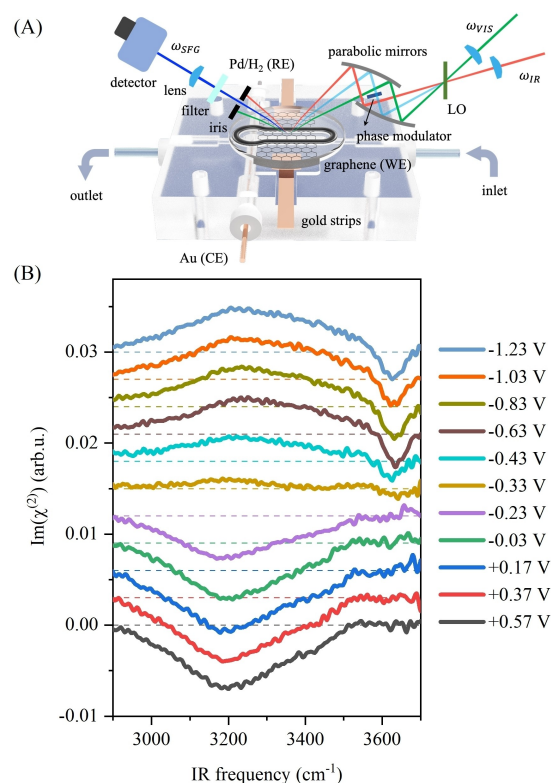
Figure 1. O–H stretching spectra at the CaF$_2$-supported graphene/water interface measured by HD-SFG, at different electrochemical potentials versus Pd/H$_2$. A) Experimental setup for the in situ electrochemical HD-SFG measurements. Monolayer graphene, Pd/H$_2$ wire, and gold wire are denoted as the working electrode (WE), reference electrode (RE), and counter electrode (CE), respectively. B) The O–H stretching Im$(\chi^{(2)})$ spectra at the CaF$_2$-supported graphene/water interface under various applied voltages. We used 1 mM NaClO$_4$ aqueous solution. The spectra are offset for clarity. The dashed lines indicate the zero line.

the CaF$_2$-supported graphene/water interface. The net charge can be obtained from the differential spectra, $\Delta\chi^{(2)}$, at different ion concentrations based on the electric double-layer model (For details, see Supporting Information-Section 5.1).[25,26,34] The Im$(\Delta\chi^{(2)})$ spectra are shown in Figure 2A, while the obtained σ_{net} is displayed in Figure 2B.[25,26] σ_{net} decreases nonlinearly from $+23$ mC m^{-2} to -14 mC m^{-2} when we change the potential from $+0.57$ V to -1.23 V. Remarkably, the nonlinear change of the σ_{net} differs significantly from the variation of charges on the graphene electrode (σ_G) obtained from the Raman G-band data in Figure 2C (see Supporting Information-Section 5.2).[35,36] Assuming that σ_{net} is the sum of σ_G and the surface charge density of the CaF$_2$ substrate (σ_{CaF_2}), we obtained σ_{CaF_2}, which is displayed in Figure 2B. The nonlinear variation of σ_{CaF_2} is striking, unlike σ_G. We note that the water response to changes in the substrate's charge is very plausible, considering that the supported graphene is transparent, at least in part, in terms of substrate-water interactions (see Supporting Information-Section 6).[37,38]

The nonlinear variation of σ_{CaF_2} indicates a pseudocapacitive process occurs at the CaF$_2$-supported graphene/water interface. To obtain further insight into the interfacial
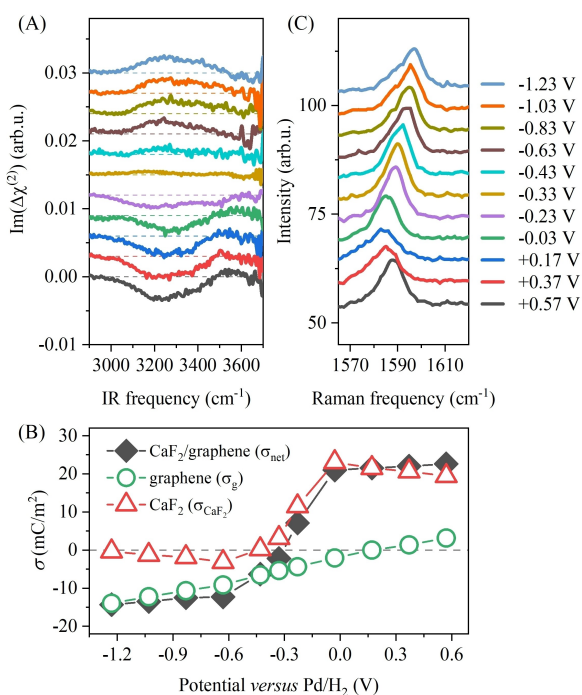
Figure 2. Surface charges at the CaF₂-supported graphene/water interface. A) The differential $\mathrm{Im}(\Delta\chi^{(2)})$ spectra obtained from taking the difference between $\chi^{(2)}$ spectra recorded at 1 mM and 100 mM NaClO₄ aqueous solutions. B) Potential-dependent net surface charge at the CaF₂-supported graphene/water interface (σ_{net} from $\Delta\chi^{(2)}$ spectra), charge density of the graphene (σ_g from Raman spectra), and inferred surface charge of the CaF₂ substrate (σ_{CaF2} from the difference). C) Raman spectra of the graphene on CaF₂ substrate, recorded under various applied potentials. The spectra in (A) and (C) are offset for clarity. The dashed lines in (A) and (B) serve as the zero line.

structure, we performed cyclic voltammetry (CV) measurements. The CV curve in Figure 3A shows two typical features: the HER region (potential below -0.23 V, $H_2O + e^- \rightarrow 1/2H_2 + OH^-$, for details, see Supporting Information-Section 7)[39,40] and the double layer region (above -0.23 V). In the double layer region, the CaF₂ substrate is positively charged at neutral pH (≈ 5.6), with its isoelectric point in the range pH 9 to 10.[41,42] In the potential region of HER, the generated OH⁻ ions will elevate the electrolyte solution's pH in the vicinity of graphene,[43–45] causing hydroxylation of the CaF₂ surface:[32,33]

$$\equiv Ca^+...H_2O \rightleftharpoons \ \equiv CaOH + H^+. \tag{1}$$
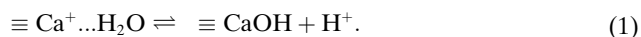
where $\equiv$ indicates a surface-bound state. The proton generated at the CaF₂/graphene interface can readily penetrate through the single-layer graphene to reach the bulk solution via (2),[46–49] leaving the Ca–O–H species on the CaF₂ surface because, unlike H⁺, OH⁻ ions cannot penetrate through the graphene to the bulk water (Experimental evidence ruling out macroscopic defects in graphene can be found in Supporting Information-Section 3.1.):[46,47]
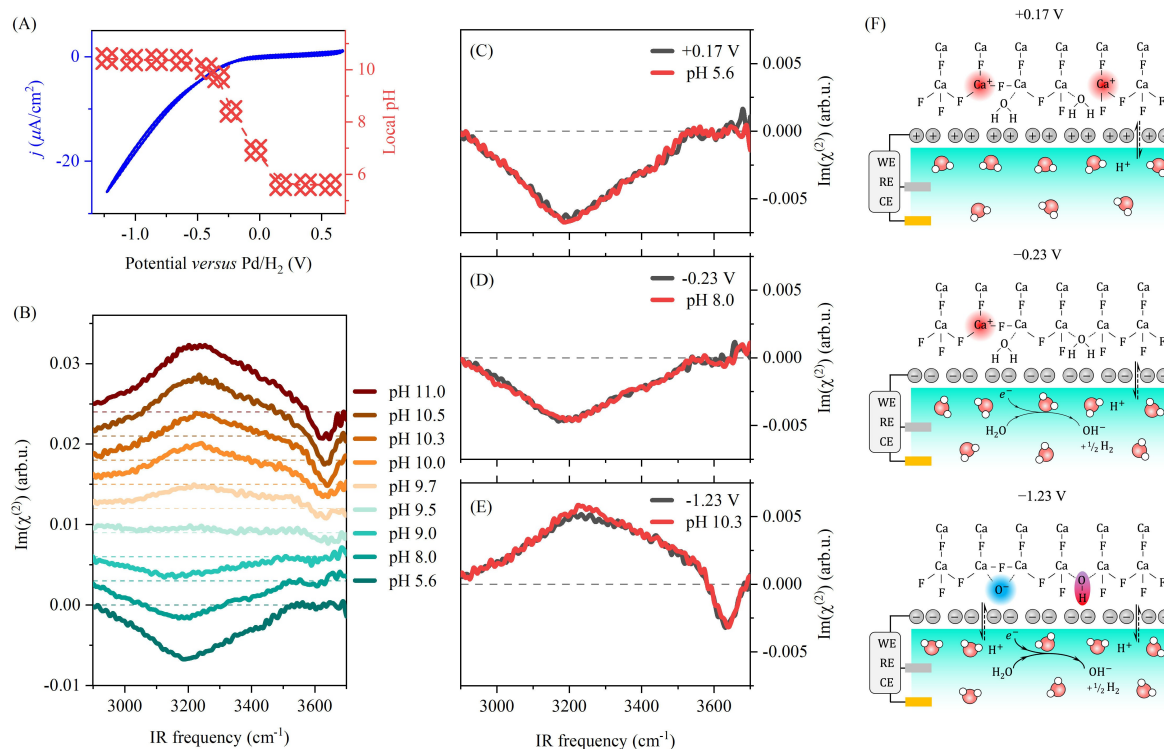
$$H^+(CaF_2/graphene) \rightleftharpoons H^+(graphene/water). \tag{2}$$
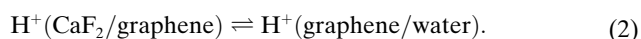
Consequently, in the potential region of HER, σ_{CaF_2} decreases dramatically (see Figure 1D) due to the hydroxylation of the CaF₂, i.e., pseudocapacitive discharging of the CaF₂. In fact, Figure 1B shows the appearance of the Ca–O–H negative peak at 3630 cm⁻¹ in the HER potential region. As such our SFG data evidences the pseudocapacitive process at the CaF₂-supported graphene/water interface.

The pseudocapacitive process at negative potentials is triggered by the local pH change at the CaF₂/graphene interface. If so, the change of the pH of the solution and varying the applied potential would have the same impact on the interfacial water. To examine this hypothesis, we measured the $\mathrm{Im}(\chi^{(2)})$ spectra under various pH conditions at the CaF₂-supported graphene/water interface. The data is displayed in Figure 3B. At bulk pH of < 9.5, the spectra exhibit a negative H-bonded O–H band. When elevating the bulk pH above 9.5, the H-bonded O–H band changes the sign from negative to positive, and a sharp negative peak at around 3630 cm⁻¹ appears, consistent with an isoelectric point between pH 9 and 10 of the CaF₂. Besides, the appearance of the 3630 cm⁻¹ peak at pH > 9.5 also confirms our assignment of the high-frequency O–H peak to the O–H stretch of Ca–O–H group on the CaF₂ surface.[32,33]

For the further direct comparison of the data measured by changing pH and by changing applied potential, we compared the spectra in Figures 3C–E. The spectra show excellent agreement in not only the lineshape but also the amplitude. These results verify that the applied potential on the graphene induces local pH change at the CaF₂/graphene interface, which induces the pseudocapacitive charging/discharging of CaF₂ and is responsible for the change in the water organization on the graphene surface.

Considering that charged graphene hardly affects water's response (for details, see Supporting Information-Section 6), we can estimate the local pH at the CaF₂/graphene interface from a comparison of the $\mathrm{Im}(\chi^{(2)})$ spectra measured by changing bulk pH and those by changing the potential. The obtained correspondence of the applied potential and local pH is shown in Figure 3A, which is correlated according to the integrated peak intensity of the H-bonded O–H band and the Ca–O–H peak (for details, see Supporting Information-Section 8). The inferred pH value saturates at increasingly low potential below -0.63 V. We expect pH to increase continuously with increasing negative potential. We tentatively assign the observed saturation to the limited number of water molecules confined between the graphene and CaF₂ (See Supporting Information-Section 3.2) as a reactant in the chemical reaction (1), limiting that reaction. In any case, it is consistent that applying a negative potential to the graphene promotes the dissociation of the water molecules confined in the CaF₂/graphene interface. Generated protons penetrate through graphene to the bulk water and recombine with OH⁻ at the graphene/water interface elevating the local pH at the CaF₂/graphene interface, and giving rise to the pseudocapacitive charging/discharging of the CaF₂. These molecular pictures are schematically depicted in Figure 3F.

In summary, we employed surface-specific spectroscopy to study water at the CaF₂-supported electrified graphene/water interface, and gain molecular-level insight into the pseudocapa-

Figure 3. Local pH change at the CaF$_2$-supported graphene/water interface. A) Cyclic voltammogram of the graphene electrode on CaF$_2$. We used 1 mM NaClO$_4$ aqueous solution, and the scan rate was set to 50 mV s^{-1}. Deduced local pH values at various applied potentials are also plotted. B) The O−H stretching Im$(\chi^{(2)})$ spectra at the CaF$_2$-supported graphene/water interface at various pH conditions. These spectra are offset for clarity. (C, D, and E) Comparison of the applied potential effect and pH effect on the O−H stretching Im$(\chi^{(2)})$ spectra. F) Schematic diagram of the CaF$_2$-supported graphene/water interface in a 1 mM NaClO$_4$ aqueous solution. At +0.17 V, no chemical reaction occurs at the graphene/water interface, CaF$_2$ substrate is positively charged. At −0.23 V, HER starts to occur, and OH$^-$ ions accumulate at the graphene/water interface, elevating the local pH. Adsorbed OH$^-$ ions reduce the positive surface charges on CaF$_2$. At more negative potentials, −1.23 V for example, interfacial chemical equilibria (1) and (2) shift to the right, causing a nearly neutral CaF$_2$ surface and the formation of Ca−O−H.

citive behavior and interfacial water molecules' arrangement near the electrified graphene electrode. We found that the Im$(\chi^{(2)})$ spectra change non-linearly vs. applied potential. The variation of the SFG spectra under the applied potentials resembles the variation of the SFG spectra under varying pH conditions, manifesting that the applied potential on the graphene triggers the dissociation of water molecules confined between the graphene sheet and CaF$_2$ substrate, changing the local pH at the CaF$_2$/graphene interface. Such pH change subsequently induces the pseudocapacitive charging/discharging of the CaF$_2$ substrate. Our molecular-level details of interfacial water structure and the pseudocapacitive behavior at the electrode/water interface are relevant for a wide range of scientific and technological systems such as water desalination, biosensing, energy storage, and catalysis.

Supporting Information

More details about the sample preparation/characterization, electrochemical cell, Raman and HD-SFG measurements can be found in the Section 1–3 of the Supporting Information. More results regarding the dynamics, reversibility, reproducibility and generality of the pseudocapacitive process are also given in Section 9–11, respectively.

Conflict of Interest

The authors declare no conflict of interest.

Data Availability Statement

The data that support the findings of this study are available from the corresponding author upon reasonable request.

[1] G. Gonella, E. H. G. Backus, Y. Nagata, D. J. Bonthuis, P. Loche, A. Schlaich, R. R. Netz, A. Kühnle, I. T. McCrum, M. T. M. Koper, M. Wolf, B. Winter, G. Meijer, R. K. Campen, M. Bonn, *Nat. Chem. Rev.* **2021**, *5*, 466–485.

[2] I. Ledezma-Yanez, W. D. Z. Wallace, P. Sebastián-Pascual, V. Climent, J. M. Feliu, M. T. Koper, *Nat. Energy* **2017**, *2*, 17031.

[3] J. Chmiola, *Science* **2006**, *313*, 1760–1763.

[4] P. Srimuk, X. Su, J. Yoon, D. Aurbach, V. Presser, *Nat. Rev. Mater.* **2020**, *5*, 517–538.

[5] M. E. Suss, V. Presser, *Joule* **2018**, *2*, 10–15.

[6] S. Boyd, K. Ganeshan, W.-Y. Tsai, T. Wu, S. Saeed, D. Jiang, N. Balke, A. C. T. van Duin, V. Augustyn, *Nat. Mater.* **2021**, *20*, 1689–1694.

[7] Y.-H. Wang, S. Zheng, W.-M. Yang, R.-Y. Zhou, Q.-F. He, P. Radjenovic, J.-C. Dong, S. Li, J. Zheng, Z.-L. Yang, G. Attard, F. Pan, Z.-Q. Tian, J.-F. Li, *Nature* **2021**, *600*, 81–85.

[8] T. Cheng, L. Wang, B. V. Merinov, W. A. Goddard, *J. Am. Chem. Soc.* **2018**, *140*, 7787–7790.

[9] S. Fleischmann, J. B. Mitchell, R. Wang, C. Zhan, D. Jiang, V. Presser, V. Augustyn, *Chem. Rev.* **2020**, *120*, 6738–6782.

[10] C. Chen, Y. Wen, X. Hu, X. Ji, M. Yan, L. Mai, P. Hu, B. Shan, Y. Huang, *Nat. Commun.* **2015**, *6*, 6929.

[11] J. B. Mitchell, W. C. Lo, A. Genc, J. LeBeau, V. Augustyn, *Chem. Mater.* **2017**, *29*, 3928–3937.

[12] S. Pezzotti, A. Serva, F. Sebastiani, F. S. Brigiano, D. R. Galimberti, L. Potier, S. Alfarano, G. Schwaab, M. Havenith, M.-P. Gaigeot, *J. Phys. Chem. Lett.* **2021**, *12*, 3827–3836.

[13] C.-S. Hsieh, M. Okuno, J. Hunger, E. H. G. Backus, Y. Nagata, M. Bonn, *Angew. Chem. Int. Ed.* **2014**, *53*, 8146–8149; *Angew. Chem.* **2014**, *126*, 8284–8288.

[14] Y. Tian, J. Hong, D. Cao, S. You, Y. Song, B. Cheng, Z. Wang, D. Guan, X. Liu, Z. Zhao, X.-Z. Li, L.-M. Xu, J. Guo, J. Chen, E.-G. Wang, Y. Jiang, *Science* **2022**, *377*, 315–319.

[15] Y. Zhang, H. B. de Aguiar, J. T. Hynes, D. Laage, *J. Phys. Chem. Lett.* **2020**, *11*, 624–631.

[16] A. Montenegro, C. Dutta, M. Mammetkuliev, H. Shi, B. Hou, D. Bhattacharyya, B. Zhao, S. B. Cronin, A. V. Benderskii, *Nature* **2021**, *594*, 62–65.

[17] A. Ge, K. Inoue, S. Ye, *J. Chem. Phys.* **2020**, *153*, 170902.

[18] A. Sayama, S. Nihonyanagi, Y. Ohshima, T. Tahara, *Phys. Chem. Chem. Phys.* **2020**, *22*, 2580–2589.

[19] A. M. Gardner, K. H. Saeed, A. J. Cowan, *Phys. Chem. Chem. Phys.* **2019**, *21*, 12067–12086.

[20] F. Tang, T. Ohto, S. Sun, J. R. Rouxel, S. Imoto, E. H. G. Backus, S. Mukamel, M. Bonn, Y. Nagata, *Chem. Rev.* **2020**, *120*, 3633–3667.

[21] S. Nihonyanagi, J. A. Mondal, S. Yamaguchi, T. Tahara, *Annu. Rev. Phys. Chem.* **2013**, *64*, 579–603.

[22] Y. R. Shen, *Nature* **1989**, *337*, 519–525.

[23] Y. R. Shen, V. Ostroverkhov, *Chem. Rev.* **2006**, *106*, 1140–1154.

[24] M. Bonn, Y. Nagata, E. H. G. Backus, *Angew. Chem. Int. Ed.* **2015**, *54*, 5560–5576; *Angew. Chem.* **2015**, *127*, 5652–5669.

[25] T. Seki, X. Yu, P. Zhang, C.-C. Yu, K. Liu, L. Gunkel, R. Dong, Y. Nagata, X. Feng, M. Bonn, *Chem* **2021**, *7*, 2758–2770.

[26] Y.-C. Wen, S. Zha, X. Liu, S. Yang, P. Guo, G. Shi, H. Fang, Y. R. Shen, C. Tian, *Phys. Rev. Lett.* **2016**, *116*, 016101.

[27] R. R. Nair, P. Blake, A. N. Grigorenko, K. S. Novoselov, T. J. Booth, T. Stauber, N. M. R. Peres, A. K. Geim, *Science* **2008**, *320*, 1308–1308.

[28] Y. Xu, Y.-B. Ma, F. Gu, S.-S. Yang, C.-S. Tian, arXiv:2207.08149 [physics.chem-ph], **2022**.

[29] S. Yang, X. Zhao, Y.-H. Lu, E. S. Barnard, P. Yang, A. Baskin, J. W. Lawson, D. Prendergast, M. Salmeron, *J. Am. Chem. Soc.* **2022**, *144*, 13327–13333.

[30] L. B. Dreier, Z. Liu, A. Narita, M.-J. van Zadel, K. Müllen, K.-J. Tielrooij, E. H. G. Backus, M. Bonn, *J. Phys. Chem. C* **2019**, *123*, 24031–24038.

[31] T. Ohto, H. Tada, Y. Nagata, *Phys. Chem. Chem. Phys.* **2018**, *20*, 12979–12985.

[32] R. Khatib, E. H. G. Backus, M. Bonn, M.-J. Perez-Haro, M.-P. Gaigeot, M. Sulpizi, *Sci. Rep.* **2016**, *6*, 24287.

[33] K. A. Becraft, G. L. Richmond, *Langmuir* **2001**, *17*, 7721–7724.

[34] P. E. Ohno, H. Wang, F. M. Geiger, *Nat. Commun.* **2017**, *8*, 1032.

[35] S. Das Sarma, S. Adam, E. H. Hwang, E. Rossi, *Rev. Mod. Phys.* **2011**, *83*, 407–470.

[36] J. Yan, Y. Zhang, P. Kim, A. Pinczuk, *Phys. Rev. Lett.* **2007**, *98*, 166802.

[37] D. Kim, E. Kim, S. Park, S. Kim, B. K. Min, H. J. Yoon, K. Kwak, M. Cho, *Chem* **2021**, *7*, 1602–1614.

[38] C.-J. Shih, M. S. Strano, D. Blankschtein, *Nat. Mater.* **2013**, *12*, 866–869.

[39] I. T. McCrum, M. Koper, *Nat. Energy* **2020**, *5*, 891–899.

[40] V. Grozovski, S. Vesztergom, G. G. Láng, P. Broekmann, *J. Electrochem. Soc.* **2017**, *164*, E3171.

[41] J. D. Miller, J. B. Hiskey, *J. Colloid Interface Sci.* **1972**, *41*, 567–573.

[42] S. Assemi, J. Nalaskowski, J. D. Miller, W. P. Johnson, *Langmuir* **2006**, *22*, 1403–1405.

[43] M. C. O. Monteiro, M. T. M. Koper, *Curr. Opin. Electrochem.* **2021**, *25*, 100649.

[44] A. T. Kuhn, C. Y. Chan, *J. Appl. Electrochem.* **1983**, *13*, 189–207.

[45] A. Veligura, P. J. Zomer, I. J. Vera-Marun, C. Józsa, P. I. Gordiichuk, B. J. van Wees, *J. Appl. Phys.* **2011**, *110*, 113708.

[46] S. Hu, M. Lozada-Hidalgo, F. C. Wang, A. Mishchenko, F. Schedin, R. R. Nair, E. W. Hill, D. W. Boukhvalov, M. I. Katsnelson, R. A. W. Dryfe, I. V. Grigorieva, H. A. Wu, A. K. Geim, *Nature* **2014**, *516*, 227–230.

[47] S. Bukola, Y. Liang, C. Korzeniewski, J. Harris, S. Creager, *J. Am. Chem. Soc.* **2018**, *140*, 1743–1752.

[48] J. Xu, H. Jiang, Y. Shen, X.-Z. Li, E. G. Wang, S. Meng, *Nat. Commun.* **2019**, *10*, 3971.

[49] J. L. Achtyl, R. R. Unocic, L. Xu, Y. Cai, M. Raju, W. Zhang, R. L. Sacci, I. V. Vlassiouk, P. F. Fulvio, P. Ganesh, D. J. Wesolowski, S. Dai, A. C. T. van Duin, M. Neurock, F. M. Geiger, *Nat. Commun.* **2015**, *6*, 6539.

Communications

Communications

Y. Wang, T. Seki, X. Liu, X. Yu, C.-C. Yu,
K. F. Domke, J. Hunger, M. T. M. Koper,
Y. Chen,* Y. Nagata,*
M. Bonn* ———————— **e202216604**

Direct Probe of Electrochemical Pseudoca-
pacitive pH Jump at a Graphene Electrode

Using surface-specific heterodyne-de-
tected sum-frequency generation, we
probe the structure and orientation of
interfacial water at a graphene electrode
and find phase transition-like changes.
We attribute it to local pH change-
induced pseudocapacitive charging/dis-
charging of the CaF_2 substrate of the
graphene electrode. Our work evidences
the molecular-level effects of pseudoca-
pacitive charging at an electrode/aque-
ous electrolyte interface.